17th International Conference on Environmental Science and Technology

Athens, Greece, 1 to 4 September 2021

Magnetic $CoFe_2O_4$@carbon yolk-shell nanoparticles as catalysts for the catalytic wet peroxide of paracetamol

SANTOS SILVA A.[1], GUARI N.[1,2], DIAZ DE TUESTA J.L.[1], POTTKER W.[2], YASSUE CORDEIRO P.[2], and GOMES H.T.[1,*]

[1]Centro de Investigação de Montanha (CIMO), Instituto Politécnico de Bragança, Campus de Santa Apolónia, 5300-253 Bragança, Portugal

[2]Federal Technological University of Paraná (UTFPR), Avenida dos Pioneiros 3131, 86036-370, Londrina, PR, Brazil

*corresponding author:
e-mail: htgomes@ipb.pt

Abstract. This work focuses the use of carbon-coated magnetic cobalt ferrite nanoparticles as catalysts for catalytic wet peroxide oxidation (CWPO) of the emerging pollutant paracetamol. A magnetic core composed of $CoFe_2O_4$ is developed by a sol-gel method. The core is subsequently coated with a formaldehyde-resorcinol resin and TEOS, further carbonized at 600 ºC, and etched with NaOH to create a yolk-shell structure denoted as $CoFe_2O_4$@void@C. XRD, TEM, and FTIR analysis revealed that the uncoated core is composed by a $CoFe_2O_4$ cubic spinel structure with a crystallite size of 53 nm calculated using the W-H method, matching very well the average size observed by TEM (53.51 ± 4.2 nm). Comparing the performances of $CoFe_2O_4$@void@C and of the bare $CoFe_2O_4$ in the CWPO of paracetamol, TOC removals of 46 and 58% are obtained respectively after 24 h of reaction. An empirical kinetic model based on second-order and autocatalytic expressions was developed to suitably describe the decomposition of H_2O_2 and the removal of paracetamol using $CoFe_2O_4$@void@C as catalyst.

Keywords: $CoFe_2O_4$ nanoparticles, CWPO, emerging pollutant, paracetamol, carbon-coated

1. Introduction

Due to their importance in catalysis, ferrite nanoparticles, such as $CoFe_2O_4$, have been intensively investigated (Ribeiro et al. 2017). Characteristics like remarkable chemical stability, large magnetic anisotropy and predominantly ferromagnetic behavior (Ribeiro et al. 2019; Ribeiro et al. 2017), contribute to the suitability of ferrites when used as heterogeneous catalysts. The main advantage is the easy separation of the catalyst from the water matrices at the end of treatment with high recovery of the material upon application of a magnetic field (Ribeiro et al. 2019; Ribeiro et al. 2017).

The present work aims to develop catalyst composites constituted of yolk-shell cobalt ferrite nanoparticles $CoFe_2O_4$@void@C for application in catalytic wet peroxide oxidation (CWPO) of water streams containing the model pollutant paracetamol. In addition, an empirical kinetic model' was developed to predict the decomposition of H_2O_2 and the removal of paracetamol.

2. Methodology

2.1 Synthesis of $CoFe_2O_4$ yolk-shell nanoparticles

The magnetic core ($CoFe_2O_4$) was synthesized according to the Sol-gel methodology described by Giannakopoulou, Kontegeorgakos and Kordas (Giannakopoulou et al. 2002). The carbon-based coating was performed following the methodology described in previous a work (Rodrigues et al. 2018). The $CoFe_2O_4$ goes through a process based on reactions with resorcinol, ammonia, TEOS, and formaldehyde to produce polymer-coated nanoparticles, resulting in graphene-based magnetic nanoparticles (GbMNPs) with a yolk-shell nanostructure, denoted as $CoFe_2O_4$@void@C.

2.2 CWPO experiments

Batch CWPO runs with paracetamol as model pollutant were performed in a stirred glass reactor. The reactor was loaded with 100 mL of paracetamol solution (100 $mg.L^{-1}$) and acidified until pH 3.5 employing H_2SO_4. 158 µL of a 30%w/v peroxide solution (472.4 $mg{\cdot}L^{-1}$) was then added. The controller maintained the temperature at 80 °C. The samples for analysis were periodically withdrawn at selected times from 5 to 1440 min, in triplicate. The samples were used to analyze PCM degradation, H_2O_2 consumption and TOC.

2.3 Characterization techniques

Structural characterization and average crystallite size were measured by X-ray Diffraction (XRD) using Cu-K_α radiation ($\lambda = 0.15$ nm) in a Bruker D8 Discover diffractometer. Transmission Electron Microscopy (TEM) was performed in an H-9000 instrument operating at 300 kV. ImageJ software (NIH, Bethesda, MD, USA) was used to estimate the size of the magnetic

nanoparticles. Fourier Transform Infrared Spectroscopy (FTIR) spectra of the $CoFe_2O_4$@void@C sample were recorded on a Perkin Elmer FT-IR spectrophotometer UATR two infrared spectrophotometer, with a resolution of 4 cm^{-1}.

3. Results and discussion

3.1 Characterization of the materials

Figure 1 shows the XRD patterns of the core $CoFe_2O_4$ powders and of $CoFe_2O_4$@void@C. As can be observed, the diffraction peaks of the XRD pattern can be indexed to $CoFe_2O_4$ cubic spinel structures with space group Fd-3m (JCPDS Card No 00-001-1121). After coating, the catalyst structure remained the same, as shown by the characteristic peaks.

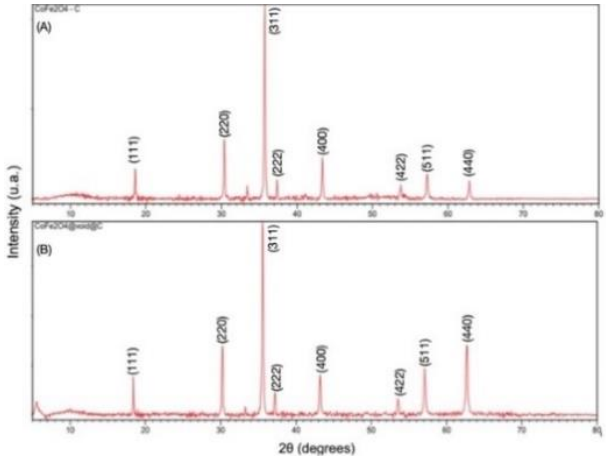

Figure 1. XRD diffractograms of the (A) core $CoFe_2O_4$ and of (B) $CoFe_2O_4$@void@C

In particular, the crystallite size of the prepared $CoFe_2O_4$ powders is 53 nm, as calculated by the Williamson-Hall method (W-H) (Nath et al. 2020). The TEM image presented in Figure 2a) shows the bare cobalt ferrite core synthesized through the sol-gel method with an average size of 53.51 ± 4.2 nm, in agreement with the value obtained by the W-H method from the XRD spectrum. The observed agglomeration is related to the ferromagnetic characteristics of the sample. By the shape and morphologies of $CoFe_2O_4$@void@C observed in Figure 2b), the lighted shadowy border evidences the coating of the magnetic nanoparticles and the cobalt ferrite core shelled by a carbon-based layer, as observed elsewhere (Ribeiro et al. 2017; Rodrigues et al. 2018).

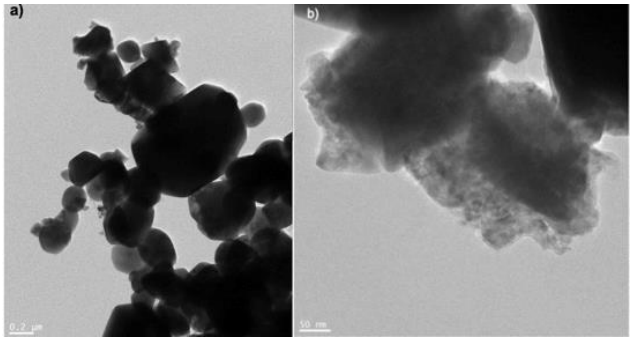

Figure 2. TEM image of the: (a) Magnetic core ($CoFe_2O_4$); (b) $CoFe_2O_4$@void@C

As expected, the increment of the number of carbon-based precursors (resorcinol, formaldehyde, and TEOS) in relation to a fixed mass of the magnetic core provided an increase of the carbon-based shell thickness, which resulted in particles with average sizes of 59 ± 8.1 nm.

The bands of the FTIR spectra (Figure 3) of $CoFe_2O_4$@void@C were compared and analyzed according to the literature of cobalt ferrite nanomaterials (Bagade et al. 2017; Wang et al. 2014). The band at 589 cm^{-1}, confirms the metal oxide in the spinel structure due to the stretching vibrations of metal oxide in the octahedral group complex Co(II)-O^{2-} of the cobalt ferrite phase.

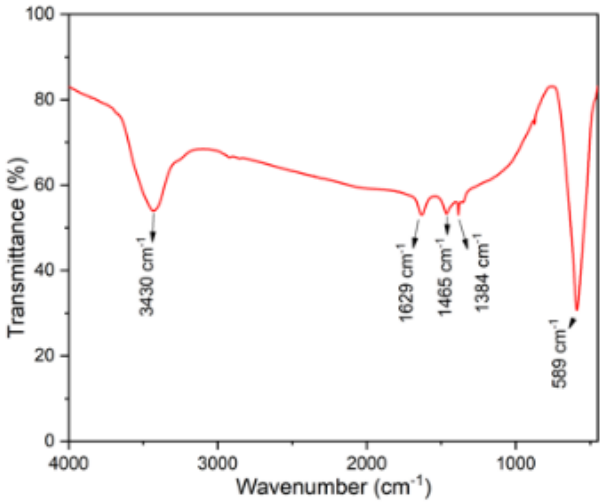

Figure 3. FTIR spectra of the $CoFe_2O_4$@void@C nanoparticles

3.2 CWPO

In order, to evaluate the efficiency of the $CoFe_2O_4$ magnetic core and of $CoFe_2O_4$@void@C, the concentrations of PCM, H_2O_2, and TOC were followed during the reaction time. To confirm the activity of the catalysts, a non-catalytic run, and pure adsorption tests were conducted at the same operating conditions.

As observed, both materials are active in the CWPO of PCM. The decomposition of H_2O_2, shown in Figure 4(a), achieved values of 10, 68, and 85% after 24 h of reaction in the non-catalytic run, and in the runs with the catalysts $CoFe_2O_4$ and $CoFe_2O_4$@void@C, respectively.

Regarding the conversion of PCM, Figure 4(b) reveals that the best-tested material is $CoFe_2O_4$@void@C, showing 99.5% of conversion after 6 h of reaction. As can be observed in Figure 4(c), the materials show higher conversions of TOC, agreeing with the conversion results obtained for paracetamol and H_2O_2. The core $CoFe_2O_4$ and $CoFe_2O_4$@void@C achieved mineralization values of 46 and 58%, respectively, after 24 h of reaction.

From the data of HPLC analysis, the absence of paracetamol adsorption after 24 h was observed. The best performance of $CoFe_2O_4$@void@C as catalyst when compared with the uncoated ferrite can be explained by the higher degree of crystallinity of the hybrid coated ferrite, as inferred from the peaks in the XRD pattern of the $CoFe_2O_4$@void@C sample, that increases significantly when compared to those of $CoFe_2O_4$.

$CoFe_2O_4$@void@C also has a higher surface area, which also contributes to superior catalysis.

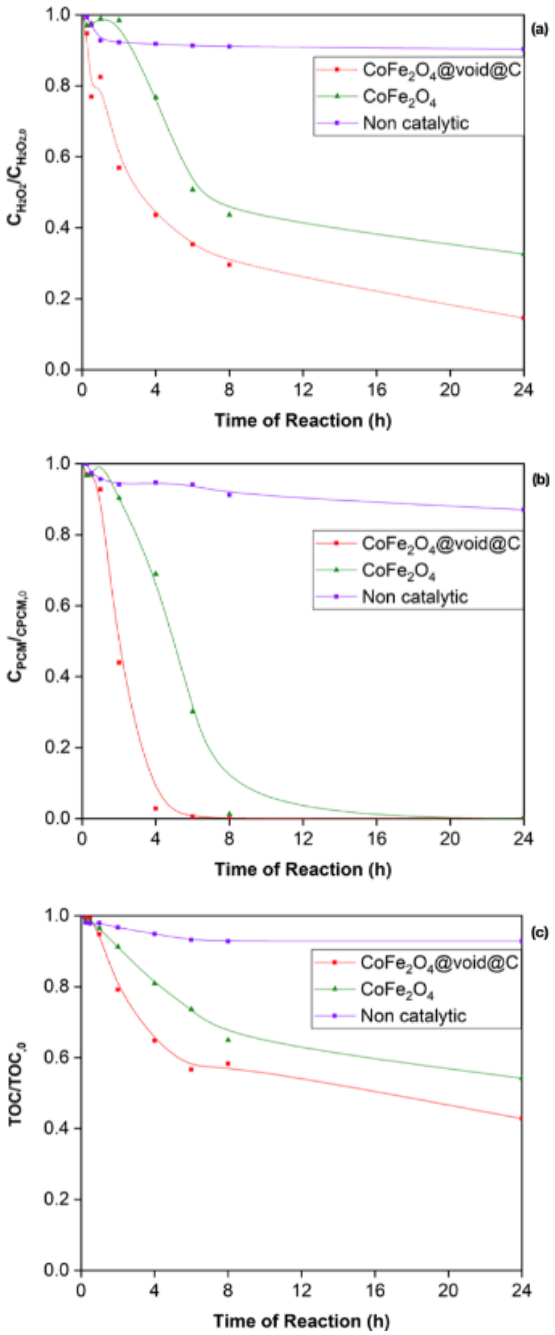

Figure 4. Normalized concentrations of (a) H_2O_2, (b) PCM and (c) TOC.

The determination of iron leached from the catalysts to the reaction solution was done after each CWPO run (24 h of reaction). As expected, the $CoFe_2O_4$@void@C material with the carbon-coated achieved a better result (iron leaching of 1.59 $mg \cdot L^{-1}$) when compared to the uncoated ferrite which had an iron leaching of 2.54 $mg \cdot L^{-1,}$ value above the limit concentration of 2 $mg \cdot L^{-1}$ of iron in water established by law.

3.3. Kinetic Modeling

To interpret the role of the oxidation reactions in the CWPO process, the kinetic results were modeled considering the system as a batch reactor of constant volume and perfect mixing, where an irreversible reaction occurs, and that the composition of the aliquot taken at a given time was identical to the internal composition of the reactor at that time. It was also considered that adsorption was negligible in the whole process. Different reaction rate equations have been proposed to fit the experimental data (Figures 5 and 6), namely first order, pseudo-first order, second order for each species and an autocatalytic-power-law kinetic model developed to predict the observed induction period and the dependence on the consumption of H_2O_2.

Due to lack of monitoring of the oxidation intermediates resulting from the oxidation of the model contaminant, only the rate of disappearance of PCM and H_2O_2 can be defined according to their concentrations, without taking into account the stoichiometry of the multiple reactions that can occur simultaneously, as shown in Eq. 1.

$$C_8H_9NO_2 + H_2O_2 \rightarrow \text{non identified oxidized products} + CO_2 + H_2O \quad (1)$$

The kinetic study was done following the methodology proposed in previous works (Diaz de Tuesta et al. 2020; Diaz de Tuesta et al. 2017). The numerical integration of the rate equations presented in Figures 5 and 6, with the initial conditions $C_{PCM} = C_{PCM,0}$, $C_{H2O2} = C_{H2O2,0}$ at $t = 0$ was solved by using the software Python v3.7 to minimize the sum of squared errors (SSE) of the relative concentration of each compound i ($rc_i = C_i/C_{i,0}$) between the experimental (exp) and predicted (model) values, as given in Eq. 2.

$$SSE = \sum_{n=1}^{N} (rc_{exp\ i,n} - rc_{model\ i,n})^2 \quad (2)$$

Regarding the disappearance of H_2O_2, the proposed model N°3 obtained a good representation of the values with a determination factor equal to 0.98 (Figure 5).

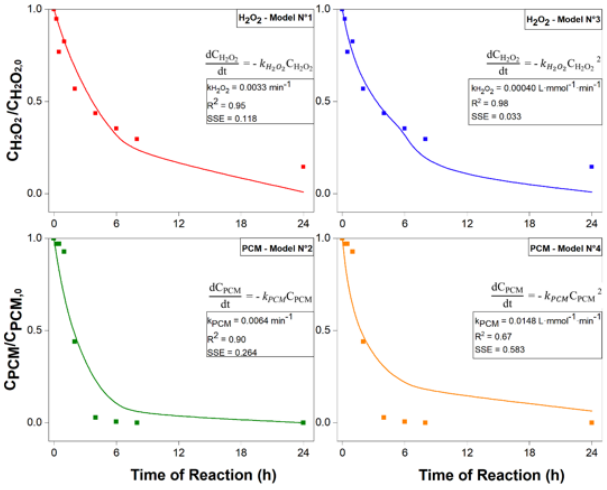

Figure 4. Experimental (symbols) and predicted (lines) concentrations of H_2O_2 (models 1 and 3) and PCM (models 2 and 4).

The initial low-activity period of paracetamol can be well explained by the autocatalytic model, with a determination factor equal to 0.99, model N° 5 (Figure 6).

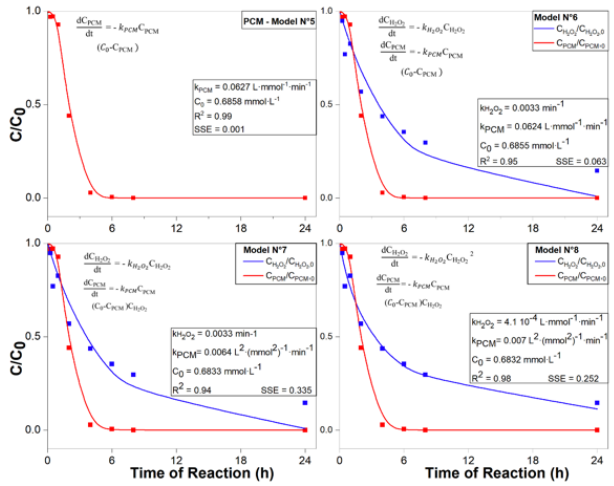

Figure 5. Experimental (symbols) and predicted (lines) concentrations of H_2O_2 and PCM

Subsequently, the best models for the pollutants and oxidants were related together and the constant C_0 was determined. It is important to highlight that the value C_0 did not change significantly regardless of the proposed experimental models (0.6858, 0.6855, 0.6833, and 0.6832 mmol·L^{-1} for the models 5, 6, 7, and 8, respectively).

4. Conclusions

Based on the premise of optimizing yolk-shell magnetic nanoparticles for application as catalysts in CWPO, this work considered the synthesis of $CoFe_2O_4$@void@C materials. XRD, TEM, and FTIR revealed that the core is composed by a $CoFe_2O_4$ cubic spinel structure with space group Fd-3m, with a crystallite size of 53 nm, calculated using the W-H method which is in agreement with the average size observed by TEM (53.51 ± 4.2 nm). The average size of the hybrid coated ferrite nanoparticles increases to 58.7 ± 8.1 nm due to the coating introduced.
The treatment of waters containing paracetamol is promising when considering the CWPO process with $CoFe_2O_4$@void@C as catalyst. The CWPO runs conducted revealed that over half of the paracetamol is converted in less than two hours of reaction. The CWPO of paracetamol with $CoFe_2O_4$@void@C lead to a mineralization value of 58%. The $CoFe_2O_4$@void@C succeeds in avoiding iron leaching and proved to be a stable catalyst, the amount of iron at the end of the reaction being equal to 1.59 mg·L^{-1}.
The CWPO of PCM with the $CoFe_2O_4$@void@C catalyst can be well-described by an empirical kinetic model composed of a second-order and an autocatalytic expression to describe the decomposition of H_2O_2 and PCM, respectively. In this sense, it is possible to predict the induction period, which takes place in the process.

5. Acknowledgements

This work is a result of Project "RTChip4Theranostics - Real time Liver-on-a-chip platform with integrated micro(bio)sensors for preclinical validation of graphene-based magnetic nanocarriers towards cancer theranostics", with the reference NORTE-01-0145-FEDER-029394, supported by Norte Portugal Regional Operational Programme (NORTE 2020), under the Portugal 2020 Partnership Agreement, through the European Regional Development Fund (ERDF); and CIMO (UIDB/00690/2020) through FEDER under Program PT2020.

References

Bagade A.A., Ganbavle V.V., Mohite S.V., Dongale T.D., Sinha B.B., Rajpure K.Y. (2017), Assessment of structural, morphological, magnetic and gas sensing properties of $CoFe_2O_4$ thin films, *Journal of Colloid and Interface Science*, **497**,181-192.

Diaz de Tuesta J.L., Quintanilla A., Casas J.A., Morales-Torres S., Faria J.L., Silva A.M.T., Gomes H.T. (2020), The pH effect on the kinetics of 4-nitrophenol removal by CWPO with doped carbon black catalysts, *Catalysis Today*, **356**,216-225.

Diaz de Tuesta J.L., Quintanilla A., Casas J.A., Rodriguez J.J. (2017), Kinetic modeling of wet peroxide oxidation with a carbon black catalyst, *Applied Catalysis B: Environmental*, **209**,701-710.

Giannakopoulou T., Kompotiatis L., Kontogeorgakos A., Kordas G. (2002), Microwave behavior of ferrites prepared via sol–gel method, *Journal of Magnetism and Magnetic Materials*, **246**,360-365.

Nath D., Singh F., Das R. (2020), X-ray diffraction analysis by Williamson-Hall, Halder-Wagner and size-strain plot methods of CdSe nanoparticles- a comparative study, *Materials Chemistry and Physics*, **239**,122021.

Ribeiro R.S., Gallo J., Bañobre-López M., Silva A.M.T., Faria J.L., Gomes H.T. (2019), Enhanced performance of cobalt ferrite encapsulated in graphitic shell by means of AC magnetically activated catalytic wet peroxide oxidation of 4-nitrophenol, *Chemical Engineering Journal*, **376**,120012.

Ribeiro R.S. et al. (2017), Hybrid magnetic graphitic nanocomposites towards catalytic wet peroxide oxidation of the liquid effluent from a mechanical biological treatment plant for municipal solid waste, *Applied Catalysis B: Environmental*, **219**,645-657.

Rodrigues R. et al. (2018), A Tailor-Made Protocol to Synthesize Yolk-Shell Graphene-Based Magnetic Nanoparticles for Nanomedicine, *C*, **4**,55.

Wang B., Gao C., Wang W., Kong F., Zheng C. (2014), TGA-FTIR investigation of chemical looping combustion by coal with $CoFe_2O_4$ combined oxygen carrier, *Journal of Analytical and Applied Pyrolysis*, **105**,369-378.